Parallel Symmetric Immobile DNA Junctions as Substrates for *E. coli* RuvC Holliday Junction Resolvase†

Ruojie Sha,‡ Furong Liu,‡ Hiroshi Iwasaki,§ and Nadrian C. Seeman*,‡

Department of Chemistry, New York University, New York, New York 10003, and Division of Molecular and Cellular Biology, Graduate School of Integrated Systems, Yokohama City University, 1-7-29, Suehiro-cho, Tsurumi-ku, Yokohama, Kanagawa 230-0045, Japan

Received April 30, 2002; Revised Manuscript Received July 16, 2002

ABSTRACT: RuvC is a well-characterized Holliday junction resolvase from *E. coli*. The presence of symmetry in its preferred recognition sequence leads to ambiguity in the position of the crossover point in the junction, because a symmetric junction can undergo branch migration. Symmetric immobile junctions are junctions that contain such symmetric sites, but are prevented from migrating by their physical characteristics. RuvC activity had been analyzed previously by traditional symmetric immobile junctions, in which the helix axes are held antiparallel in a double-crossover motif. Bowtie junctions are branched four-arm molecules containing 5′,5′ and 3′,3′ linkages at their crossover points. A new type of symmetric immobile junction can be made by flanking the crossover point of a Bowtie junction with a symmetric sequence. The junction is immobile because mobility would lead to pairing between parallel, rather than antiparallel, nucleotide pairs. In contrast to conventional Holliday junctions and their analogues, the Bowtie junction assumes a parallel, rather than antiparallel, helical domain conformation, offering a new type of substrate for Holliday junction resolvases. Here, we report the digestion of Bowtie junctions by RuvC. We demonstrate that Bowtie junctions can function as symmetric immobile junctions in this system. We also show that RuvC cleaves antiparallel junctions much more efficiently than parallel junctions, where the protein can bind (and cleave) only one site at a time. These data suggest that the presence of two binding sites leads to communication between the two subunits of the enzyme to increase its activity.

The Holliday (*1*) junction is the most prominent DNA intermediate in genetic recombination. It is known to be involved in site-specific recombination (*2*−*4*), and it is likely to be involved in homologous recombination (*5*). The life cycle of the Holliday junction in recombination is illustrated in Figure 1, which depicts the process in junctions with both parallel and antiparallel conformations. The first step, shown at the left of the drawing, is the formation of the junction (II) from two pieces of DNA containing homology (I). The branch point of the Holliday junction is flanked typically by regions of dyad (homologous) sequence symmetry; this symmetry enables the branch point to relocate through an isomerization known as branch migration (e.g., *6*). The product of branch migration (III) is illustrated in the step to the right of formation. Proceeding to the right, the Holliday junction may undergo another conformational change, known as crossover isomerization. This rearrangement reverses the helical and crossover strands (IV), and it is known to be spontaneous (*7*). The junctions then may be cleaved (V) by resolvases, such as endonuclease VII (*8*) or RuvC (*9*), and religated (VI).

The symmetry that enables branch migration makes it difficult to study the features of Holliday junctions. For example, it is difficult to characterize the crossover preferences of Holliday junctions whose sequence at the branch point is not fixed. To overcome this problem, we developed a symmetric immobile junction (SIJ)[1] (*10*) based on double-crossover molecules (*11*). In this system, two junctions are separated by one or one and a half helical turns; one of these junctions is flanked by a symmetric sequence, but the other is immobile because it is not flanked by a symmetric sequence. At this close separation, the immobility of the asymmetric junction translates into immobility for the symmetric junction, because its migration would alter significantly the twist in the intervening region. We have used these SIJ molecules to characterize the thermodynamics of crossover isomerizations (*12*) and of branch migratory minima (*13*) associated with symmetric sequences. Recently,

† This research has been supported by Grant GM-29554 from the National Institute of General Medical Sciences, Grant N00014-98-1-0093 from the Office of Naval Research, Grants DMI-0210844, EIA-0086015, DMR-01138790, and CTS-0103002 from the National Science Foundation, Grant F30602-01-2-0561 from DARPA/AFSOR to N.C.S., and by Grants-in Aid for Scientific Research on Priority Areas (C) "Genome Biology" from the Ministry of Education, Culture, Sports, Science and Technology of Japan to H.I.

* To whom correspondence should be addressed. E-mail: ned.seeman@nyu.edu, Tel: 212-998-8395, Fax: 212-260-7905.

‡ New York University.

§ Yokohama City University.

[1] Abbreviations: Bowtie junction, Holliday junction analogue containing 5′,5′ and 3′,3′ linkages in its crossover strands; BSA, bovine serum albumin; DTT, dithiothreitol; EDTA, ethylenediaminetetraacetic acid; SIJ, symmetric immobile junction; SIJ1K, symmetric immobile junction of the first kind; SIJ2K, symmetric immobile junction of the second kind; TAEMg, solution containing 40 mM Tris, pH 8.0, 20 mM acetic acid, 2 mM EDTA, and 12.5 mM magnesium acetate; TBE, solution containing 100 mM Tris, pH 8.3, 89 mM boric acid, and 2 mM EDTA.

10.1021/bi020319r CCC: $22.00
Published on Web 08/15/2002

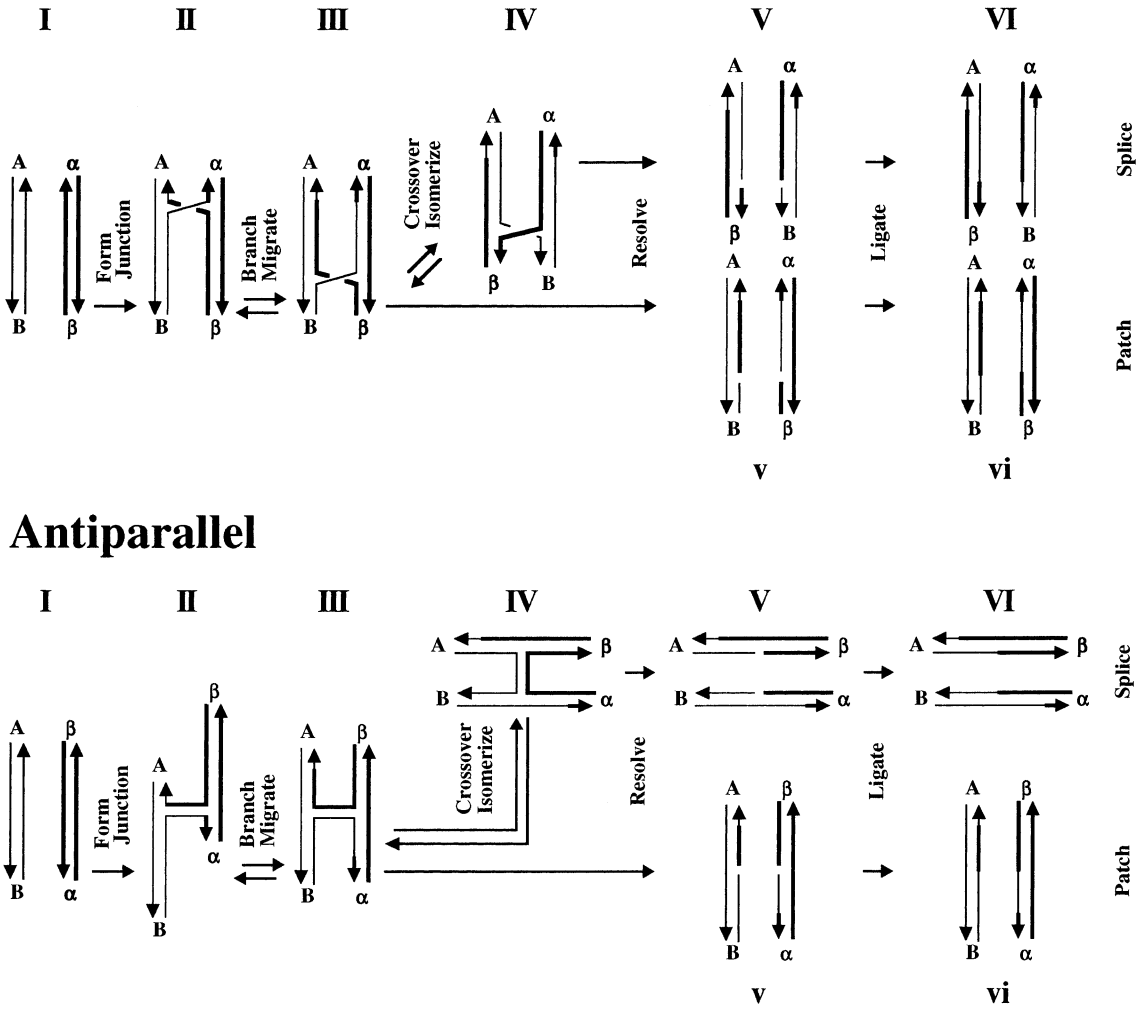

FIGURE 1: Formation and resolution of the Holliday structure in genetic recombination. The process is illustrated both in the commonly shown parallel conformation, and also in the antiparallel conformation, suggested by physical data; it proceeds from the left to the right. Each of the possible stages is labeled with capital or small Roman numerals. In the first stage, I, two homologous double helices of DNA align with each other. The two strands of each duplex are indicated by the two pairs of lines terminated by arrowheads, which indicate the 3′ ends of the strands. Strands are distinguished by their thickness. Each of these two homologous regions carries a flanking marker, A and B in the strands on the left, and α and β on the right. After the first step, the homologous pairs have formed a Holliday intermediate, II, by exchanging strands. Note that the two crossover strands are composite strands with both a thick and a thin portion formed through any of a number of possible mechanisms. The homologous 2-fold sequence symmetry of this structure permits it to undergo the iterative isomerization process, branch migration; movement in the direction indicated results in structure III. The Holliday intermediate may or may not undergo the crossover isomerization process to produce structure IV, in which the crossover and noncrossover strands are switched. Although indicated as separate, the crossover isomerization process could be a feature of branch migration (*8*). If crossover isomerization occurs an odd number of times, resolution by cleavage of the crossover strands yields structure V, but structure v results if crossover isomerization occurs an even number of times (including 0) before cleavage. Ligation of v generates a patch recombinant, vi; this is a pair of linear duplex DNA molecules containing heteroduplex DNA because of branch migration, but which have retained the same flanking markers. Ligation of VI yields splice recombinant molecules, that have exchanged flanking markers.

we have also used them to establish the feasibility of branch migration in antiparallel junctions (*14*) and to characterize the location of the branch point when it cleaved by RuvC (*15*). The key fault involving these SIJ molecules is that their interdomain angle is constrained to be exactly antiparallel, unlike the angles measured in solution (*16*, *17*), on surfaces (*18*), or in the most representative crystals (*19*), which are 40−60° from that orientation. As a substrate, a further fault of the SIJs is that recognition sites may be occluded in the molecule, which is known to be quite rigid (*20*).

Recently, we have described Bowtie junctions (*21*), Holliday-like junctions containing 5′,5′ and 3′,3′ linkages at their crossover sites. We have characterized these molecules in solution, and find that they are similar to conventional Holliday junctions in that they stack their four arms to produce two helical domains. However, they differ from conventional junctions in that the orientation of these helical domains changes by about 50°, so that they are in the parallel, rather than antiparallel, range of conformations (*21*, *22*). A special feature of Bowtie junctions is that the unusual linkages appear to confer immobility on these junctions, even if the sequence flanking the junction is symmetric: As shown in Figure 2, branch migration would entail replacing antiparallel nucleotide pairs with parallel pairs, an arrangement unlikely to be favorable (*23*). In addition, we have shown that crossover isomerization does not occur in Bowtie

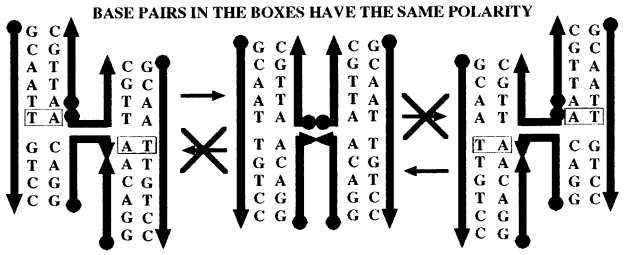

FIGURE 2: Inability of Bowtie junctions to undergo branch migration. A Bowtie junction with a symmetric sequence is shown in the center portion of this drawing. Filled circles indicate 5′ ends, and arrowheads indicate 3′ ends. The two conventional strands have the same sequence. The top crossover strand contains a 5′,5′ linkage, and the bottom crossover strand contains a 3′,3′ linkage. Were the junction to undergo branch migration, parallel nucleotide pairs would be formed (shown in boxes), rather than antiparallel nucleotide pairs, so the junction is not expected to undergo branch migration.

junctions; the unusual linkages are always on the crossover strands, regardless of sequence (*21*). Thus, Bowtie junctions might be used as SIJs of a second kind (SIJ2K). Although imperfect in their own way, SIJ2Ks provide different types of constraints from the first kind of SIJ (SIJ1K): There is no enforcement of planarity on the double-helical domains, but the angle between helical domains is different from that seen for conventional junctions; furthermore, the linkage in the crossover strands is unnatural.

Here, we demonstrate that symmetric Bowtie junctions are immobile, and we illustrate their utility by examining how they serve as substrates for *E. coli* RuvC. We have constructed a symmetric branched junction containing 5′,5′ and 3′,3′ linkages in the junction position and analyzed this structure in solution by using hydroxyl radical autofootprinting (*24*) and Cooper-Hagerman/Lilley gel mobility experiments (*25*). Those experiments show that the symmetric Bowtie junction is parallel and immobile. We further demonstrate that the antiparallel junction is a far better substrate for RuvC than a parallel junction, suggesting communication between the subunits. In addition, we find in this system that the sequence outside the RuvC preferred sequence 5′-ATTG-3′ (*9, 26*) appears to affect the cleavage efficiency of the enzyme.

MATERIALS AND METHODS

Synthesis and Purification of DNA. All DNA molecules used in this study were synthesized on an Applied Biosystems 380B automatic DNA synthesizer, removed from the support, and deprotected using routine phosphoramidite procedures (*27*). Strands containing 3′,3′ and 5′,5′ linkages have been synthesized by substituting 5′ phosphoramidites (Glen Research) for conventional 3′ phosphoramidites in half the synthesis. Yields are not significantly reduced by switching polarities. All strands were purified by polyacrylamide gel electrophoresis.

Formation of Symmetric Bowtie Junction Molecules. The component strands of symmetric Bowtie junction molecules (60 pmol) were dissolved to a concentration of 3 μM in 20 μL of a solution containing 40 mM Tris, pH 8.0, 20 mM acetic acid, 2 mM EDTA, and 12.5 mM magnesium acetate (TAEMg) and heated to 90 °C for 5 min, and then cooled to 65 °C for 15 min, 37 °C for 15 min, room temperature (ca. 22 °C) for 20 min, and 4 °C for 20 min. The cooling protocol was interrupted at the appropriate stages for experiments to be performed at higher temperatures.

Hydroxyl Radical Autofootprinting Analysis. Individual strands of the molecules were radioactively labeled, and were additionally gel-purified from a 20% denaturing polyacrylamide gel. Each of the labeled strands (approximately 10 pmol in TAEMg) was annealed to a 4-fold excess of the unlabeled complementary strand, or it was annealed to the complex, as described above, or it was left untreated as a control, or it was treated with sequencing reagents (*28*) for a sizing ladder. Hydroxyl radical cleavage of the samples took place at 4 °C for 100 s (*29*), with modifications noted by Churchill et al. (*24*). The reaction was stopped by addition of thiourea. The samples were ethanol-precipitated, dried, dissolved in a formamide/dye mixture, and loaded directly onto a 14% polyacrylamide sequencing gel containing 8.3 M urea. Autoradiograms were quantitated using a BioRad GS-250 Molecular Imager.

Enzymatic Reactions. (*A) Kinase Labeling.* Two picomoles of an individual strand of DNA were dissolved in 10 μL of a solution containing 50 mM Tris·HCl, pH 7.6, 20 μM spermidine, 10 mM $MgCl_2$, 15 mM dithiothreitol (DTT), and 0.2 mg/mL nuclease-free bovine serum albumin (BSA) (U.S. Biochemical), and mixed with 1 μL of 1.25 mM [γ-^{32}P]ATP (10 μCi/μL) and 3 units of T4 polynucleotide kinase (USB) for 2 h at 37 °C. The reaction was stopped by phenol extraction and ethanol precipitation of DNA.

(B) Ligations. Ten units of T4 polynucleotide ligase (U.S. Biochemical) in 30 μL of a buffer supplied by the manufacturer were added to 10 pmol of each strand, and the reaction was allowed to proceed at 16 °C. for 10−16 h. The reaction was stopped by heat inactivation, followed by gel purification.

(C) RuvC Digestions. RuvC was prepared as described previously (*30*). Twenty picomoles of the DNA complex at a concentration of 1 μM, annealed as above to 37 °C, was combined with 60 pmol (3 μM) of RuvC and allowed to incubate for 45 min in 20 μL of the RuvC reaction buffer (10 mM $MgCl_2$, 1 mM dithiothreitol, 0.01% bovine serum albumin, 20 mM Tris, pH 8.0, and 5% glycerol). The reaction was stopped by adding 2 μL of 500 mM EDTA, heating to 90 °C for 5 min, drying down, and adding 10 μL of denaturing gel loading dye.

Denaturing Polyacrylamide Gel Electrophoresis. These gels contained 8.3 M urea and were run at 55 °C. Gels contained 6−20% acrylamide (19:1, acrylamide:bisacrylamide). The running buffer consisted of 100 mM Tris, pH 8.3, 89 mM boric acid, 2 mM EDTA (TBE). The sample buffer consisted of 10 mM NaOH, 1 mM EDTA, 90% formamide, containing 0.1% Xylene Cyanol FF tracking dye. Gels were run on an IBI model STS 45 electrophoresis unit at 70 W (50 V/cm) constant power and dried onto Whatman 3MM paper, and the distribution of each species was quantitated using a BioRad GS-250 Molecular Imager.

Nondenaturing Polyacrylamide Gel Electrophoresis. Gels contained 8−20% acrylamide (19:1, acrylamide:bisacrylamide). DNA was suspended in 10−25 μL of TAEMg, and the solution was hybridized as described above. Samples were then brought to a final volume of 20 μL and a concentration of 1 μM, with a solution containing TAEMg, 50% glycerol, and 0.02% each of Bromophenol Blue and Xylene Cyanol FF tracking dyes. Gels were run on a Hoefer

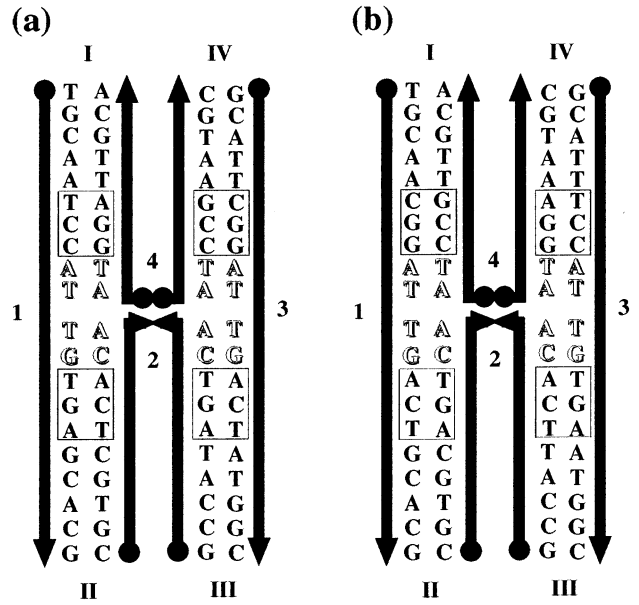

FIGURE 3: Schematic drawing of symmetric Bowtie junctions used in this work. Filled circles represent 5′ ends, and arrowheads represent 3′ ends. (a) The original Bowtie junction directly converted from J1. The RuvC recognition sequence flanking the crossover point is shown in inverse shading. The sequences that differentiate the two helical domains are boxed. These are reversed in (b). The sequences in the boxes are switched between arms I and IV as well as between arms II and III.

SE-600 gel electrophoresis unit at 11 V/cm at 4 °C, and stained with Stainsall dye.

Gel Retardation Experiments. A solution containing 20 pmol (1 μM) of symmetric immobile junction, labeled on strand 3, was incubated with inactive mutant D7E of RuvC (*17*) at 4 °C for 15 min in 20 μL of RuvC binding buffer, a variant of the reaction buffer in which 1 mM $MgCl_2$ replaces 10 mM $MgCl_2$. Gels containing 8% acrylamide (19:1, acrylamide/bisacrylamide) were buffered with 44.5 mM Tris, pH 8.0, 44.5 mM boric acid, and 1 mM EDTA. The sample buffer was the same as the running buffer, except that it contained 5% glycerol and 0.1% Xylene Cyanol FF tracking dye. Electrophoresis was performed on a Hoefer SE-600 unit at 4 °C for 4 h at 8.3 V/cm. The gels were electrophoresed for 0.5 h under the same conditions prior to loading. Gels were dried onto Whatman 3MM paper and were quantitated using a BioRad GS-250 Molecular Imager.

RESULTS

Sequence Design. The basis for the design of symmetric Bowtie junctions studied here is the asymmetric Bowtie junction (*21*) which was modeled on the well-characterized J1 junction (*31, 32*) and used in previous studies. For this work, we have simply inserted the *E. coli* RuvC preferred sequence 5′-ATTG-3′ (*9, 26*) into the helical strands at the junction-flanking position and have kept the outside arms the same. We place the center of the preferred sequence at the branch point, in keeping with our previous finding that this is where it is located when cleavage occurs (*15*). We have also constructed a longer arm version of this molecule for Cooper−Hagerman experiments (*25*), whose sequences have been selected by using the program SEQUIN (*33*). The junction-flanking sequences of the molecules used are shown in Figure 3.

Hydroxyl Radical Autofootprinting. Hydroxyl radical autofootprinting is a biochemical tool that has been used for preliminary structural characterization of a variety of unusual DNA motifs, including branched junctions (*24*), SIJ1Ks (*10*), antijunctions and mesojunctions (*34, 35*), double-crossover molecules (*36*), triple-crossover molecules (*37*), and asymmetric Bowtie junctions (*21*). The experiment compares the quantitative hydroxyl radical cleavage pattern of each strand paired with its duplex complement to the pattern of the same strand complexed in the unusual motif. The duplex pattern serves to control for sequence effects, and provides a baseline of known structure with which to compare the pattern in the unusual motif. If the cleavage pattern of the strand in the two complexes is the same, the inference is that the strand has adopted a helical structure in the unusual motif. The nucleotides flanking crossover points characteristically evince a protection from cleavage, relative to the double-helical control (*24*). In the case of strand 2, containing a 3′,3′ linkage, the complementary strand used to establish the duplex pattern contains a 5′,5′ linkage opposite the 3′,3′ linkage; similarly, the duplex complement to strand 4, containing a 5′,5′ linkage, contains a 3′,3′ linkage opposite that point.

Figure 4 illustrates the hydroxyl radical autofootprinting analysis of the Bowtie junction. The pattern for each strand in the junction is compared with its pattern in a double helix. Figure 4a contains the autofootprinting pattern for a conventional mobile junction with the RuvC recognition sequence flanking its crossover point. Virtually no protection is seen, because the junction is free to migrate between five positions and to undergo crossover isomerization, as well. Figure 4b shows the autofootprinting pattern of the Bowtie junction, which differs markedly from the pattern in Figure 4a: Dramatic protection relative to duplex is visible at the nucleotides flanking the Bowtie junction crossover points on strands 2 and 4. Thus, strands 2 and 4 are likely to be the crossover strands of this molecule. This notion is supported by the absence of strong protection on strands 1 and 3, which are expected to be the helical strands. It suggests that the stacking pattern of the Bowtie junction consists of arm I stacked on arm II and arm III stacked on arm IV, thereby producing two stacking domains. Thus, the overall stacking arrangement is similar to that of the asymmetric Bowtie junction even though a symmetric sequence flanks the junction point. Protection is also visible 3−4 nucleotides 3′ to the crossover point on the noncrossover strands, as expected from model building (*38*).

Gel Mobility Studies. Hydroxyl radical autofootprinting alone does not address the relative orientation of the two helical domains. Hence, we have used Lilley's modification (*39*) of the Cooper−Hagerman (*25*) gel mobility experiment to answer this question. First, we constructed a longer (100 bp/arm) version of the symmetric Bowtie junction, including unique blunt-end restriction sites on each arm; six combinations are generated by pairwise restriction of the junction to produce a molecule in which two arms have been trimmed to 11 base pairs. Figure 5 shows the results of this experiment, which are similar to those of the asymmetric Bowtie junction (*21*). An important part of the interpretation of a Cooper−Hagerman experiment is the independence of the results from the conditions of the assays, particularly the

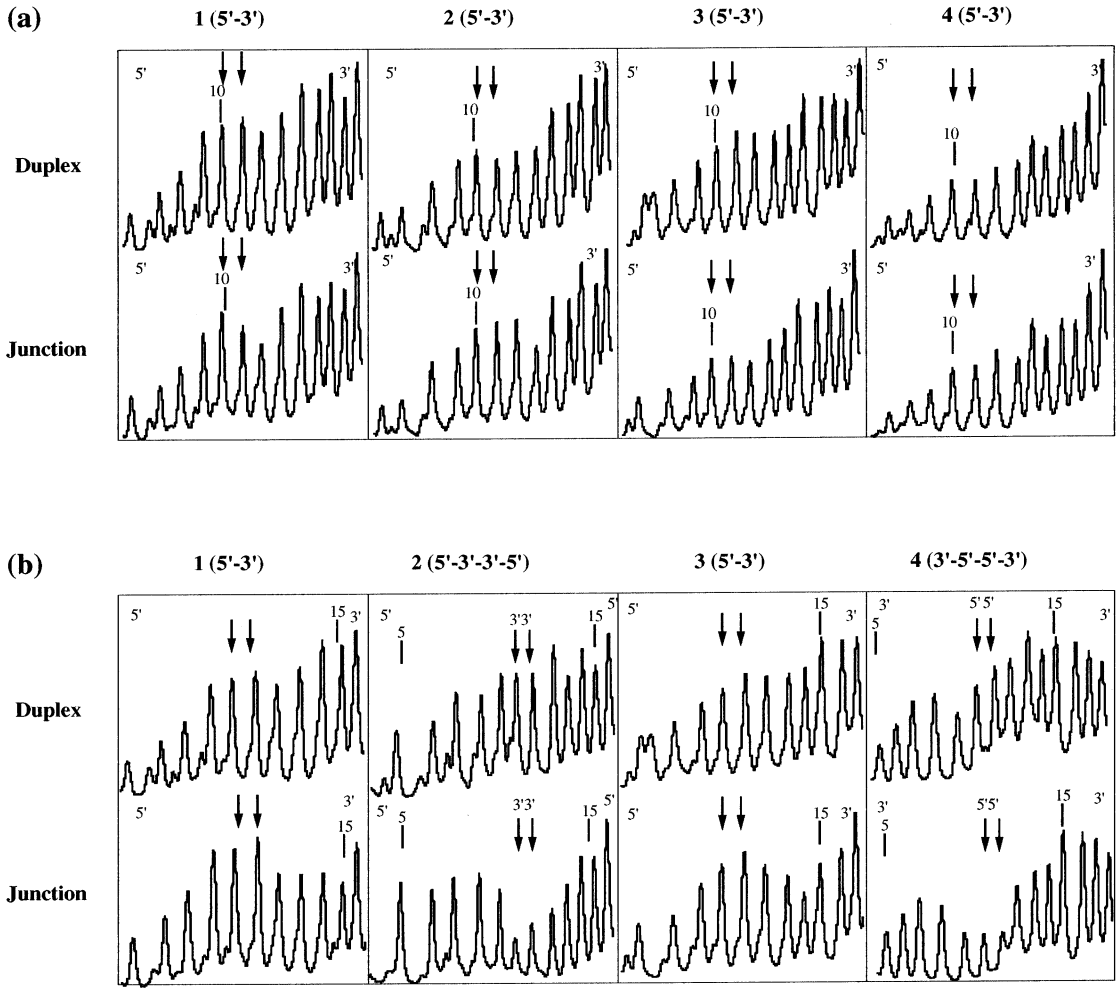

FIGURE 4: Hydroxyl radical autofootprinting of conventional (a) and Bowtie (b) junctions containing the RuvC cleavage site. The data represent scans quantitating the cleavage of strands by hydroxyl radicals. The strand in a double-helical context (labeled 'Duplex') is used as a control with which to compare the pattern of the strand in the junction. The nominal position of the crossover point is indicated by two vertical arrows. The key feature of the patterns is that the patterns of the conventional junction and its duplex are about the same, because the junction can migrate over many positions. By contrast, the crossover point in the Bowtie molecule shows characteristic protection on the crossover strands, relative to the duplex control, indicating that the branch point is fixed in this molecule.

gel percentage (*40, 41*). Figure 6 contains Ferguson plots (*42*), which establish firmly that the properties ascribed to those molecules are independent of the gel percentage. Thus, we can conclude that the orientation of the two helical domains falls within the parallel range of conformations in this symmetric Bowtie junction, similar to the orientations demonstrated in previous studies for asymmetric Bowtie junctions (*21, 22*).

Cleavage of Symmetric Bowtie Junctions by RuvC. RuvC is known to cleave the helical strands of Holliday junctions (*15, 43*), corresponding to strands 1 and 3 here. Figure 7 shows the products of RuvC cleavage of strand 1 and strand 3 of symmetric Bowtie junctions and symmetric conventional junctions. The Bowtie junction requires digestion for much longer times to obtain comparable amounts of cleavage. The Bowtie junction used above is labeled Bowtie I in Figure 7. Figure 7a shows digestion for 2 min, and Figure 7b shows digestion for 60 min. Regardless of the orientation of the helical domains of the junction, RuvC always cleaves the same position, between T and G (*15, 26*). However, the RuvC cleavage efficiency and reaction rate differ dramatically between Bowtie and conventional junctions. The conventional junction is cleaved more efficiently by RuvC than is the Bowtie junction; it is 60% digested after 2 min, whereas the Bowtie junction is cleaved 1.6−13% during the same period (see below). The difference of cleavage efficiency between Bowtie and normal junctions is not caused by the difference of their binding efficiencies. Figure 8 shows a gel retardation experiment that demonstrates that their binding efficiencies are similar. We find no super-shifting, suggesting that no multiple binding occurs. This finding confirms the previous suggestion that RuvC binding and cleavage are two separate processes (*15*).

Surprisingly, RuvC cleavage efficiency between the two helical strands (1 and 3) in the same symmetric Bowtie junction differs substantially. There are two possibilities; one is that 5′,5′ and 3′,3′ linkages have distorted the junction and have had different effects on the two helical strands; the other is that the different sequence outside the preferred symmetric sequence interacts differently with RuvC, thereby leading to different cleavage efficiencies. To distinguish these two possibilities, we have switched three base pairs just outside 5′-ATTG-3′ between the two helical domains, as shown in Figure 3b. We find that the cleavage efficiencies of strand 1 and strand 3 switch, as shown in Figure 7, where

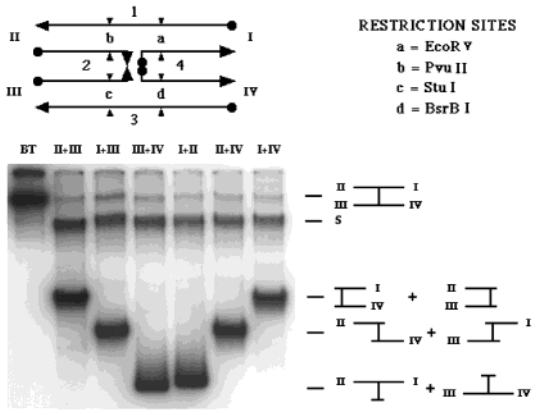

FIGURE 5: Reporter arm analyses demonstrating the parallel nature of the symmetric Bowtie junction. A nondenaturing 6% polyacrylamide gel is shown containing, from left to right, the uncleaved junction and a series of six lanes headed by the identification of the pair of arms restricted. Above the gel is a drawing of the junction, indicating the strand numbering, the arm numbering, and the positions of cleavage in a code of a−d. The code is explained to the right of the junction. To the right of the gel are schematic drawings of the migrating species. These drawings and the one at the top indicate the conformations derived from this experiment. In all of these representations, the distance between helical domains has been extended greatly so that figures can be labeled conveniently; the actual distance is only a few angstroms. 'S' represents singly cleaved junctions. In all cases, the most rapidly migrating species are those restricted in arms I+II and III+IV, confirming the domain structure established by hydroxyl radical autofootprinting. The slowest migrating species are those restricted in arms II+II and I+IV, indicating a parallel orientation of strands 1 and 3 and the domains to which they belong.

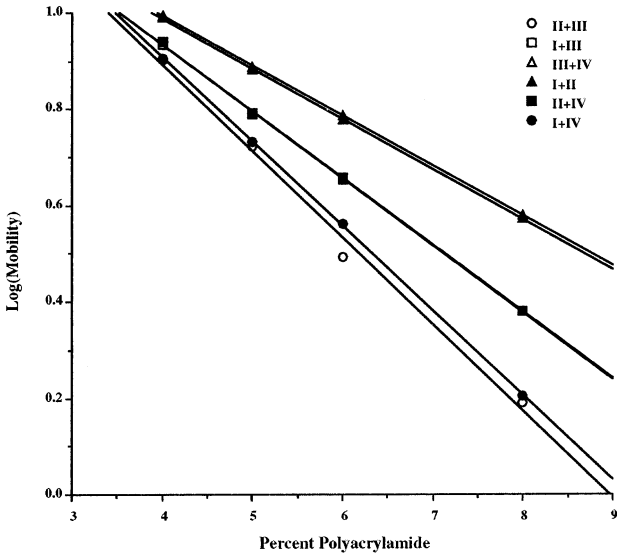

FIGURE 6: Ferguson plots of the species containing reporter arms. The purpose of these plots is to ensure that the differential mobilities seen in Figure 5 are not artifacts of the gel concentration. In each panel, the complementary pairs of reporter arms are shown with symmetrical symbols, filled and empty. In each case, the most slowly migrating species, II+III and I+IV, are visibly slower at all relevant concentrations. Likewise, I+II and III+IV are the fastest at all concentrations, confirming the domain structure.

this switched junction is labeled Bowtie II. We conclude that the sequence outside the RuvC preferred sequence 5′-ATTG-3′ affects RuvC cleavage efficiency in this system.

We see cleavage on both helical strands of the junction, although the sensitivities of the two sites are clearly a function of sequence. This observation raises an interesting

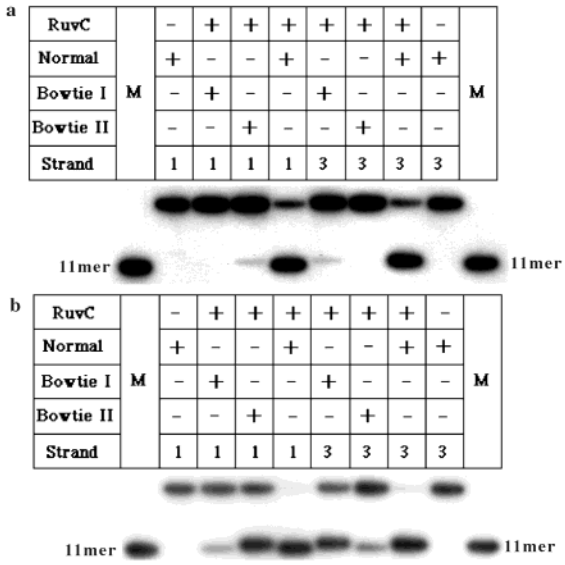

FIGURE 7: Cleavage of symmetric Bowtie junctions by RuvC. (a) Products of cleavage for 2 min. This is an autoradiogram of a 20% denaturing polyacrylamide gel. The upper panel indicates the molecules and strand number in the lanes. Strand 1 or strand 3 is end-labeled with ^{32}P-containing phosphate groups. Normal stands for the conventional junction in which 5′-ATTG-3′ sequence flanks in the branch point. Bowtie I stands for the original symmetric Bowtie junction, which is shown in Figure 3a. Bowtie II stands for the second Bowtie junction, whose sequences outside 5′-ATTG-3′ are switched, as shown in Figure 3b. From the cleavage efficiency, we conclude that the conventional junction is a better substrate for RuvC than the Bowtie junction and also that the sequence outside 5′-ATTG-3′ affects cleavage efficiency. (b) Products of cleavage for 60 min. The same conventions are used as in (a).

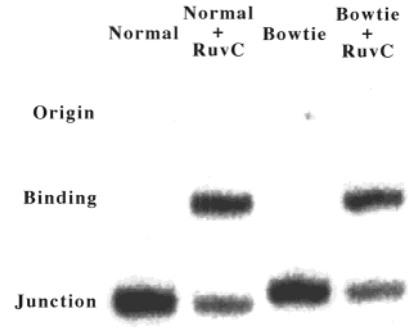

FIGURE 8: Gel retardation of symmetric Bowtie junctions by RuvC at 37 °C. This is an autoradiogram of an 12% nondenaturing gel. The first lane from the left contains the conventional junction, but lacks RuvC. The second lane contains both the conventional junction and RuvC. The third lane contains the Bowtie junction, but lacks RuvC. The fourth lane contains both the Bowtie junction and RuvC. Strand 1 is labeled in all of these molecules. The right side of the gel contains duplex controls, one with RuvC, and one without it; the duplex molecule is strand 1 of both junctions and its Watson−Crick complement. Note that the conventional junction and the Bowtie junction bind to RuvC similarly.

question. The dyad symmetry of the Bowtie junction is a parallel symmetry, where identical features appear on opposite faces of the junction; by contrast, the symmetry of the enzyme is an antiparallel symmetry (*44*), leading to symmetric features on the same face of the junction. This difference is illustrated in Figure 9, showing that it may be difficult for coordinated cleavage to occur from a single binding event. Thus, one must ask whether the cleavage on

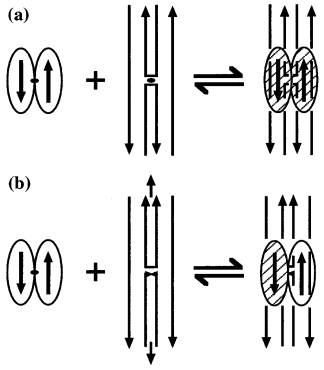

FIGURE 9: Binding of RuvC to parallel and antiparallel branched junctions. Panel a shows the binding of RuvC to an antiparallel junction. RuvC is represented as two ellipses in contact, and the symmetry element normal to the plane of the page is represented by a small filled ellipse. The symmetry element of the branched junction is illustrated similarly. When RuvC binds to the junction, the two symmetry elements can coincide so that both helical domains are in contact with a subunit of RuvC. Proper binding is illustrated by the shading of the ellipses. Panel b shows the same representation of RuvC, but shows a parallel junction. Its symmetry element is represented by the vertical arrows in the plane of the page. When the two components bind, only one of the two subunits is oriented properly to bind, as indicated by the shading of only a single ellipse. In principle, a second RuvC molecule could bind on the rear of the junction, but for clarity this molecule has not been drawn.

both strands is coordinated, or whether it is independent cleavage, perhaps caused by dissociation of the enzyme and its rebinding to the intact strand. Hence, it is important to make sure that our symmetric Bowtie junction cannot convert to another structure by a pathway involving strand dissociation. To avoid this problem, we have constructed a cyclically closed symmetric Bowtie junction by adding a hairpin to each arm of the symmetric Bowtie junction. A single cleavage event will lead to a linearized product, the full length of the cyclic molecule; a double cleavage produces a labeled fragment of roughly half-length. The result of RuvC cleavage experiments of the closed molecules is shown in Figure 10. From this 10% denaturing polyacrylamide gel, we can see clearly that lanes 4 and 6, containing the conventional junctions, show far more cleavage product than lanes 3 and 5, containing the Bowtie junctions. As in the case of the open Bowtie junctions, the conventional junctions are seen to be far better substrates for *E. coli* RuvC than Bowtie junctions. The length of cleavage products of the Bowtie junctions is about a 200-mer, the length of the whole molecule, suggesting that RuvC has cut the Bowtie junctions only once. By contrast, the length of cleavage products of conventional junctions is about a 100-mer, half of the length of the whole molecule. Thus, it is clear that RuvC has cleaved the conventional junctions twice. In the absence of further data at very short times, we cannot conclude that RuvC cleaves the conventional junctions coordinately, but the data here certainly support that idea. However, it is clear that the presence of two binding/cleavage sites on the substrate increases the rate of the reaction significantly.

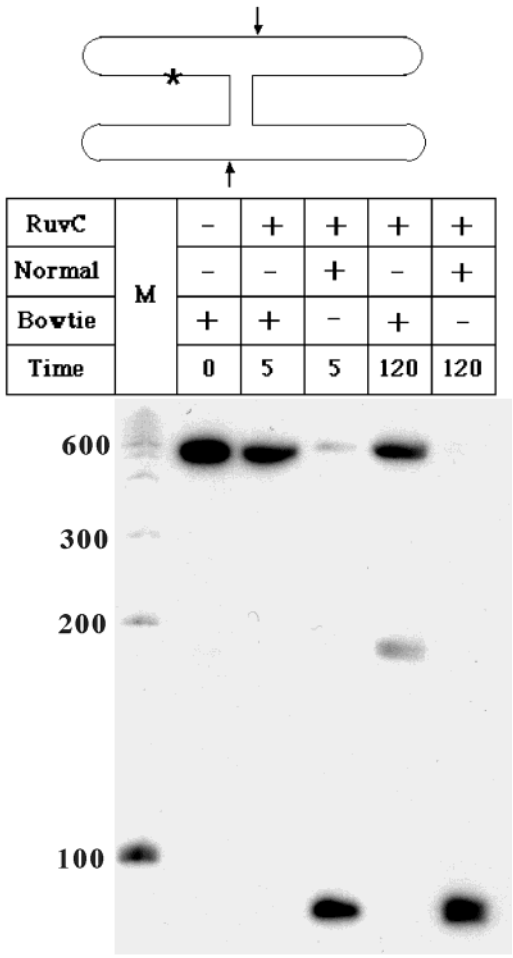

FIGURE 10: Cleavage of closed symmetric Bowtie and conventional junctions by RuvC. This is an autoradiogram of a 10% denaturing polyacrylamide gel. The Bowtie junction could be closed because hairpins were added to each arm of the junction, as shown at the top part of the figure; it was labeled by end-labeling one of the strands before the molecule was sealed shut. The lane labeled 'M' contains a series of markers. The treatment of the material in the other lanes is indicated above them. The leftmost of these lanes is a control containing a closed Bowtie junction, but lacking RuvC. Proceeding left to right, the next lane contains a closed Bowtie junction treated with RuvC for 5 min. The next lane contains a closed conventional junction treated with RuvC, also for 5 min. The last two lanes are the same, but the reaction time is 120 min. Note that the RuvC dimer digests the conventional junction to a doubly cut species (shorter product), whereas the product of Bowtie cleavage is a singly cut molecule (longer product).

DISCUSSION

Symmetric Immobile Junctions of the Second Kind. We have shown previously (*21*) that the stacking arrangements of Bowtie junctions are determined by the presence of the unusual linkage: The crossover strands will be those containing the 5′,5′ and 3′,3′ linkages. Here, we have placed the symmetric sequence 5′-ATTG-3′ in the junction position. Hydroxyl radical autofootprinting experiments demonstrate that the branch point remains immobile, thus indicating that Bowtie junctions are capable of serving as symmetric immobile junctions. The Cooper−Hagerman/Lilley gel mobility experiments confirm the parallel-like nature of the junction, even in the case where a symmetric sequence flanks the junction. As we have noted elsewhere, parallel and antiparallel define conformational semicircles, similar to 'syn' and 'anti' in nucleoside structure (45); 'antiparallel' is about 63° from ideally antiparallel (*18*), and parallel is about 68° from ideally parallel (*22*).

We have also shown that the orientations of the domains of the Bowtie junction are as flexible as those of the

conventional junction (E. Chapman, R. Sha, G.-Q. Tang, D. P. Millar, and N. C. Seeman, in preparation). Thus, we have produced a symmetric immobile junction in which the orientations of the domains are likely to be variable, removing the constraints inherent in the first type of symmetric immobile junction, based on double-crossover molecules. Nevertheless, the SIJ2K is imperfect, lacking the characteristics we would like to have in an ideal symmetric immobile junction: a relaxed antiparallel-like structure containing a fixed but symmetric sequence in which two helical domains have an orientation that reflects the natural angle that the junction wishes to adopt, in the range of 40−60°. Recently, we have developed such a symmetric immobile junction, predicated on DNA parallelograms (*18*); its properties will be reported elsewhere (S. Liao, C. Mao, S. Shuman, and N. C. Seeman, in preparation).

RuvC Cleavage of Parallel Junctions. In the crystal structure of RuvC (*44*), the enzyme forms a dimer with a 2-fold axis. Docking studies (*44*) indicate that its substrate, a DNA branched junction, should also possess a 2-fold axis, which passes through the crossover point. The symmetry of RuvC is consistent with an antiparallel junction, whose cleavage surfaces are oriented to permit both subunits to effect scission simultaneously, as suggested by Shah et al. (*46*). The 2-fold symmetry of the Bowtie junction is that of a parallel junction, so that only a single subunit can make contact with it at a time, as suggested by Figure 9. We can exclude the possibility that RuvC changes the conformation of the Bowtie junction to an antiparallel junction while binding, because in that case the strand polarities would be inappropriate for cleavage. Thus, it seems that the resolution seen with this substrate is likely to result from two RuvC dimers binding to the two sides of the Bowtie junction, possibly at different times. This arrangement would prevent it from cleaving coordinately or from having its rate enhanced by the presence of two sites of scission. This mechanism may explain why RuvC cleaves each side of the Bowtie junction with different efficiencies, in contrast to the antiparallel DNA junction, where the efficiencies appear the same for the time points measured. This suggestion is supported by the cyclic structure experiment, in which the product is a molecule that is cut only once (the longer product in Figure 10), whereas the cleavage product of the antiparallel DNA junction is doubly cut (the shorter product in Figure 10). Thus, RuvC appears capable of cleaving a junction-containing molecule that does not conform to the antiparallel structure of a conventional junction, but it is very much less efficient, and it does not cleave it in a coordinated fashion.

Mechanism of RuvC Cleavage. The key finding here relevant to the mechanism of RuvC action is that the presence of two identical available binding sites on the same substrate molecule accelerates the rate markedly. Shah et al. (*46*) have described phosphorothioate-based substrates in which RuvC cleavage occurs separately on the two sides of the junction. The gel retardation experiments performed here suggest similar affinities for the presence of the RuvC recognition sequence in both conventional and Bowtie junctions, even though only a single member of the RuvC dimer is likely to be bound to the Bowtie junction. Thus, the impact of the presence of two sites is likely to be in the cleavage step. Our data suggest that the two members of the dimer influence each other's catalytic activity, increasing it markedly when both are bound to substrate. These data support a similar conclusion drawn from different data by Shah et al. (*46*). The physical and structural basis of this acceleration is not evident at this time, and will require further experimentation.

REFERENCES

1. Holliday, R. (1964) *Genet. Res. 5*, 282−304.
2. Hoess, R., Wierzbicki, A., and Abremski, K. (1987) *Proc. Natl. Acad. Sci. U.S.A. 84*, 6840−6844.
3. Kitts, P. A., and Nash, H. A. (1987) *Nature 329*, 346−348.
4. Nunes-Duby, S. E., Matsumoto, L., and Landy, A. (1987) *Cell 50*, 779−788.
5. DasGupta, C., Wu, A. M., Kahn, R., Cunningham, R. P., and Radding, C. M. (1981) *Cell 25*, 507−516.
6. Hsieh, P., and Panyutin, I. G. (1995) *Nucleic Acids Mol. Biol. 9*, 42−65.
7. Li, X., Wang, H., and Seeman, N. C. (1997) *Biochemistry 36*, 4240−4247.
8. Mueller, J. E., Kemper, B., Cunningham, R. P., Kallenbach, N. R., and Seeman, N. C. (1988) *Proc. Natl. Acad. Sci. U.S.A. 85*, 9441−9445.
9. Shinagawa, H., and Iwasaki, H. (1996) *Trends Biochem. Sci. 21*, 107−111.
10. Zhang, S., Fu, T.-J., and Seeman, N. C. (1993) *Biochemistry 32*, 8062−8067.
11. Fu, T.-J., and Seeman, N. C. (1993) *Biochemistry 32*, 3211−3220.
12. Zhang, S., and Seeman, N. C. (1994) *J. Mol. Biol. 238*, 658−668.
13. Sun, W., Mao, C., Liu, F., and Seeman, N. C. (1998) *J. Mol. Biol. 282*, 59−70.
14. Sha, R., Liu, F., and Seeman, N. C. (2000) *Biochemistry 39*, 11514−11522.
15. Sha, R., Iwasaki, H., Liu, F., Shinagawa, H., and Seeman, N. C. (2000) *Biochemistry 39*, 11982−11988.
16. Murchie, A. I. H., Clegg, R. M., von Kitzing, E., Duckett, D. R., Diekmann, S., and Lilley, D. M. J. (1989) *Nature 341*, 763−766.
17. Eis, P., and Millar, D. P. (1993) *Biochemistry 32*, 13852−13860.
18. Mao, C., Sun, W., and Seeman, N. C.(1999) *J. Am. Chem. Soc. 121*, 5437−5443.
19. Eichman, B. F., Vargason, J. M., Mooers, B. H. M., and Ho, P. S. (2000) *Proc. Natl. Acad. Sci. U.S.A. 97*, 3971−3976.
20. Li, X., Yang, X., Qi, J., and Seeman, N. C. (1996) *J. Am. Chem. Soc. 118*, 6131−6140.
21. Sha, R., Liu, F., Bruist, M. F., and Seeman, N. C. (1999) *Biochemistry 38*, 2832−2841.
22. Sha, R., Liu, F. Millar, D. P., and Seeman, N. C. (2000) *Chem. Biol. 7*, 743−751.
23. Rentzeperis, D., Rippe, K., Jovin, T. M., and Marky, L. A. (1992) *J. Am. Chem. Soc. 114*, 5926−5928.
24. Churchill, M. E. A., Tullius, T. D., Kallenbach, N. R., and Seeman, N. C. (1988) *Proc. Natl. Acad. Sci. U.S.A. 85*, 4653−4656.
25. Cooper, J. P., and Hagerman, P. J. (1987) *J. Mol. Biol. 198*, 711−719.
26. Shah, R., Bennett, R. J., and West, S. C. (1994) *Cell 79*, 853−864.
27. Caruthers, M. H. (1985) *Science 230*, 281−285.
28. Maxam, A. M., and Gilbert, W. (1977) *Proc. Natl. Acad. Sci. U.S.A. 74*, 560−564.
29. Tullius, T. D., and Dombroski, B. (1985) *Science 230*, 679−681.
30. Saito, A., Iwasaki, H., Ariyoshi, M., Morikawa, K., and Shinagawa, H. (1995) *Proc. Natl. Acad. Sci. U.S.A. 92*, 7470−7474.
31. Seeman, N. C., and Kallenbach, N. R. (1983) *Biophys. J. 44*, 201−209.
32. Kallenbach, N. R., Ma, R.-I., and Seeman, N. C. (1983) *Nature (London) 305*, 829−831.
33. Seeman, N. C. (1990) *J. Biomol. Struct. Dyn. 8*, 573−581.
34. Du, S. M., Zhang, S., and Seeman, N. C. (1992) *Biochemistry 31*, 10955−10963.
35. Wang, H., and Seeman, N. C. (1995) *Biochemistry 34*, 920−929.
36. Fu, T.-J., and Seeman, N. C. (1993) *Biochemistry 32*, 3211−3220.

37. LaBean, T. H., Yan, H., Kopatsch, J., Liu, F., Winfree, E., Reif, J. H., and Seeman, N. C. (2000) *J. Am. Chem. Soc. 122*, 1848−1860.
38. Seeman, N. C. (1988) *J. Biomol. Struct. Dyn. 5*, 997−1004.
39. Duckett, D. R., Murchie, A. I. H., Diekmann, S., Von Kitzing, E., Kemper, B., and Lilley, D. M. J. (1988) *Cell 55*, 79−89.
40. Chen, J., and Seeman, N. C. (1991) *Electrophoresis 12*, 607−611.
41. Mueller, J. E., Du, S. M., and Seeman, N. C. (1991) *J. Am. Chem. Soc. 113*, 6306−6308.
42. Ferguson, K. A. (1964) *Metabolism 13*, 985−1002.
43. Bennett, R. J., and West, S. C. (1996) *Proc. Natl. Acad. Sci. U.S.A. 93*, 12217−12222.
44. Ariyoshi, M., Vassylyev, D. G., Iwasaki, H., Nakamura, H., Shinagawa, H., and Morikawa, K. (1994) *Cell 78*, 1063−1072.
45. Donohue, J., and Trueblood, K. N. (1960) *J. Mol. Biol. 2*, 363−371.
46. Shah, R., Cosstick, R., and West, S. C. (1997) *EMBO J. 16*, 1464−1472.

BI020319R